of the individual modes, such a rationale is not useful. For example, in this case, the symmetric CH_2 modes in each conformer occur at nearly the same frequencies so that much of their contribution to the VCD cancels, but the C*-H labeled modes are more shifted in frequency between conformers which leads to their dominating the lower frequency part of the C-H stretching region. This, again, is the nature of the force field dependence we are observing. When this fundamental limitation is kept in mind, it seems that the calculations can be viewed as being in very good agreement with the experiment subject to minor shifts in frequency. At this level, VCD could be seen as a major additional constraint in conventional force field development since the patterns observed are much more sensitive to normal mode frequencies and symmetries than is the absorption spectrum in such spectrally crowded regions.

As well as an analysis of the applicability of the LMO and FPC models and a study of their force field dependencies, we have also attempted to study the effect of charge choice on the FPC results. The results in Table I for FPC calculations all used a charge distribution that treats the axial and equatorial hydrogens and deuteriums equivalently. In this model the charge magnitudes were scaled such that the sum of the calculated dipolar strengths matched the integrated experimental values. In this approach, the $\Delta\epsilon$ values also come out to be in satisfactory agreement with experiment. This equivalent charge distribution is not seen in the population analysis of a CNDO calculation. Such a method of determining charge would indicate that the axial values should be 0.026 |e| and the equatorial values should be 0.252 |e| to effect the same scaling. FPC calculations using this charge distribution show more detailed deviations from the systematics of Table I. However, the VCD envelope found for each region is qualitatively the same as that seen in Figures 4, 6, 8, and 9. This consistency again results from summed rotational strengths, being much more consistent than those of individual modes. This is particularly evident from summing A and B symmetry C*-H and symmetric CH_2 stretch R^k values (Table II). For this CNDO charge distribution, the two conformers tend to have large VCD's that cancel each other, while the equivalent charge distribution used in the calculations reported in Table I led to both conformers having smaller R^k's which, however, added constructively. Charge effects then could lead to changes in the high-resolution VCD but, for cyclobutane, do not seem to be important in our realistially broadened VCD plots.

Two other related points deserve comment. The equivalent charge distribution was chosen because it gave a significantly better representation of the absorption line shape in the C-H region. In most of our previous studies,[12,13] the FPC-calculated absorption did not adequately reflect the distribution of dipolar strength between asymmetric and symmetric CH_2 and CH_3 modes. This is also true for these calculations, but the situation is much worse when scaled CNDO charges are used. In this latter case, the symmetric CH_2 modes have too much intensity. We feel that the large difference in the magnitude of the charge between the axial and equatorial hydrogens must be an artifact of the CNDO method. It might be noted that the FPC results consistently calculate the ϵ and $\Delta\epsilon$ values for C-D stretching to be much higher than found experimentally. This appears to be due to a line-width difference in the C-H and C-D regions.

With the above in mind, it is very interesting to note how similar the FPC and LMO results are (aside from the overall magnitude). Since the LMO uses the same CNDO method that gives rise to the unusual charge distribution above, we might conclude that redistribution effects serve to counteract the static charge distribution.

Conclusion

In summary, we have shown that the LMO and FPC models give equivalent fits to the C-H and C-D stretching mode VCD of *trans*-1,2-dideuteriocyclobutane. Improved fit can be obtained by improving the force field, but this is primarily due to change in the frequencies of individual modes rather than in their fundamental nature. As such, it would seem that the basic sense of the calculated rotational strengths is not as strongly dependent upon force fields as are the frequencies. However, in crowded spectral regions, it is imperative that both effects be accounted for to fit VCD spectra accurately. Thus, it seems that the FPC will remain a useful qualitative theoretical model for C-H stretching VCD within the constraints of conservative spectra and moderate overlap of modes. Furthermore, we feel that this molecule, dideuteriocyclobutane, will provide a hydrocarbon standard for testing further theoretical models. Extension of these studies to the mid-infrared region should further test the applicability and force field dependence of the FPC model. Such studies are underway in our laboratory.

Acknowledgment. We gratefully acknowledge the National Science Foundation (CHE81-04997) and the National Institutes of Health (GM-30147) for support of this research. We thank Professor L. Abels for assistance in obtaining the Raman spectra and the Nicolet Corp. for loan of an FT-IR spectrometer. We especially thank Professor P. Polavarapu for allowing us to use his LMO program and instructing us in its use and Professors J. Overend and L. Nafie for helpful conversations.

Registry No. *trans*-1,2-Dideuteriocyclobutane, 75156-31-9.

Mechanism for Forming Hydrogen Chloride and Sodium Sulfate from Sulfur Trioxide, Water, and Sodium Chloride

Alfred B. Anderson

Contribution from the Chemistry Department, Case Western Reserve University, Cleveland, Ohio 44106. *Received February 21, 1984*

Abstract: A molecular orbital study of sodium sulfate and hydrogen chloride formation from sulfur trioxide, water, and sodium chloride shows no activation barrier, in agreement with recent experimental work of Kohl, Fielder, and Stearns. Two overall steps are found for the process. First, gas-phase water reacts with sulfur trioxide along a pathway involving a linear O···H···O transition state yielding closely associated hydroxyl and bisulfite which rearrange to become a hydrogen sulfate molecule. Then the hydrogen sulfate molecule transfers a hydrogen atom to a surface chloride in solid sodium chloride while an electron and a sodium cation simultaneously transfer to yield sodium bisulfate and gas-phase hydrogen chloride. This process repeats. Both of these steps represent well-known reactions for which mechanisms have not been previously determined.

Sodium sulfate is a product of the reaction of combustion gases with solid sodium chloride and is, in its molten state, a powerful corrosive agent against protective oxide films on turbine blades,[1] leading to failure by "hot corrosion".[2] Recently Anderson, Hung,

0002-7863/84/1506-6262$01.50/0

and Debnath[3] have determined a mechanism for the following reaction under anhydrous conditions:

$$NaCl(s) + O_2(g) + SO_2(g) + SO_3(g) \rightarrow Na_2SO_4(s) + Cl_2(g) + SO_3(g) \quad (1)$$

They found this reaction, which has an experimentally determined activation energy of 22 kJ/mol,[4] is catalyzed by SO_3. Recent studies of Kohl et al.[5] show that when water is present at about the same mole percent concentration as sulfur trioxide (~0.1 mol % in their experiments), there is no activation barrier to sodium sulfate formation. Evidently sodium sulfate formation proceeds by a different mechanism in the presence of water, an assumption further supported by the formation of hydrogen chloride in the products.[5] The purpose of the present study is to determine a mechanism for sodium sulfate formation under hydrous conditions. The molecular orbital theory and parameters are those used previously.[6] The ASED-MO theory is based on partitioning molecular electronic charge density functions into rigid atom superposition components and a nonrigid electron delocalization bond charge part. As an atom joins another atom or a molecule the force on its nucleus due to the atom superposition densities and nuclear repulsions is easily integrated, yielding a repulsive energy component. The attractive energy component from integrating the force due to the electron delocalization density is conveniently approximated by a one-electron molecular orbital energy determined by using a Hamiltonian similar to extended Hückel. As may be seen in ref 3 and references therein, this is a generally accurate procedure for structure and reaction energy studies when used with careful selection of atomic orbital parameters. As in extended Hückel studies, the primary focus of ASED-MO studies is on the molecular orbital theory of the bonding.

It is safe to assume the reaction does not involve aqueous dissolutions of sodium chloride because of the ~600 °C reaction temperature.[5] Therefore gas-phase and solid-gas reactions are examined and a mechanism is found which has no calculated barrier. The first step involves hydrogen sulfate formation according to

$$SO_3(g) + H_2O(g) \rightarrow H_2SO_4(g) \quad (2)$$

The second step has hydrogen sulfate react with the sodium chloride surface:

$$H_2SO_4(g) + 2NaCl(s) \rightarrow 2HCl(g) + Na_2SO_4(s) \quad (3)$$

The overall reaction is the sum of (2) and (3):

$$SO_3(g) + H_2O(g) + 2NaCl(s) \rightarrow 2HCl(g) + Na_2SO_4(s) \quad (4)$$

Formation of Hydrogen Sulfate

Reaction 2 is well-known,[7] and a recent study of Sievert and Castleman indicates the activation energy is in the range of 0 to 54 kJ/mol.[8] Two reactions of interest are studied here. The first is the formation of an $H_2O{\cdot}SO_3$ adduct of 74-kJ/mol stability, which may be compared to a value of 64 kJ/mol estimated by Holland and Castleman[9] by scaling energies from a CNDO calculation. The bonding is dominated by mixing of the H_2O $3a_1$ lone-pair orbital and SO_3 3a′ orbital with the antibonding orbital

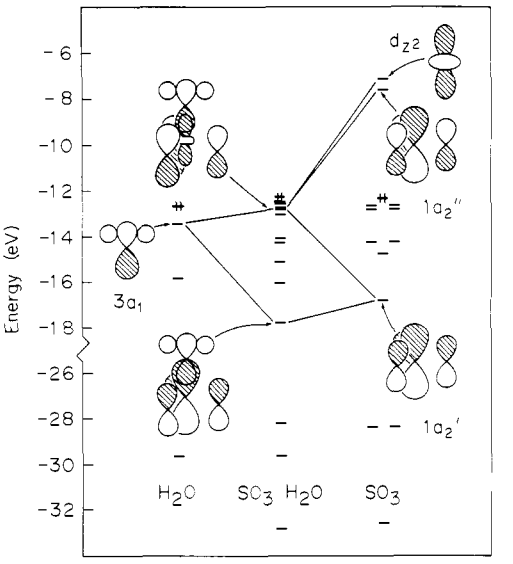

Figure 1. Donation and back-donation interactions responsible for bonding in the $H_2O{\cdot}SO_3$ adduct.

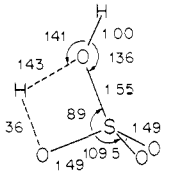

Figure 2. Transition state for $H_2O{\cdot}SO_3 \rightarrow H_2SO_4$. The S–O distance of 1.55 Å is fixed (see text). Angles optimized in 5° increments and lengths in 0.01-Å increments.

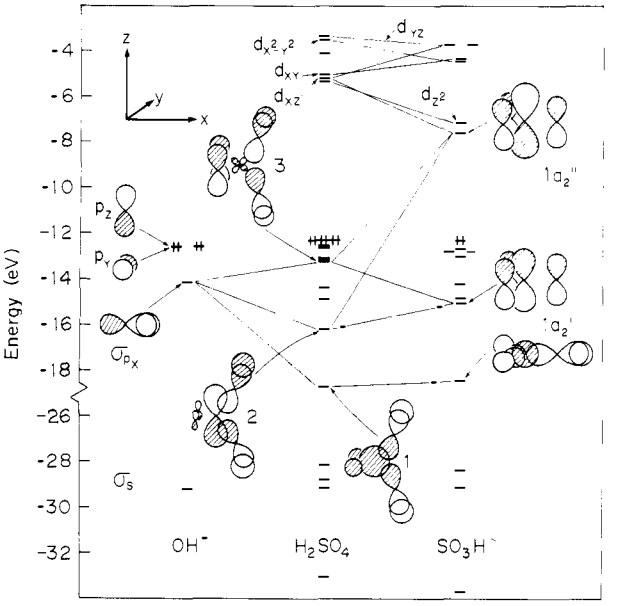

Figure 3. Correlation of OH^- and SO_3H^+ orbitals with those for H_2SO_4.

stabilized by $3a_1$ back-donation into the SO_3 $1a_2''$ orbital. On bending back the SO bonds to the tetrahedral angles, the SO distances in SO_3 increase from 1.43 to 1.49 Å and the SO distance involving H_2O is 1.6 Å. This allows the d_{z^2} orbital on sulfur to mix in. The molecular orbital correlations are shown in Figure 1. A search of the energy surface for internal hydrogen atom transfer to form hydrogen sulfate results in a barrier of ~216 kJ/mol at the transition state in Figure 2. To avoid the possibility of the adduct falling apart, this transition state is determined with the SO distance fixed at 1.55 Å. Other angles and distances are optimized. As may be seen by examining hydrogen sulfate SOH bonding orbitals in Figure 3, the transfer of a hydrogen atom so that $2OH \leftrightarrow O + OH_2$ involves considerable loss of bonding orbital

(1) Fryburg, G. C.; Kohl, F. J.; Stearns, C. A.; Fielder, W. L. *J. Electrochem. Soc.* **1982**, *129*, 571.
(2) Stringer, J. *Annu. Rev. Mater. Sci.* **1977**, *7*, 477.
(3) (a) Anderson, A. B.; Hung, S. C. *J. Am. Chem. Soc.* **1983**, *105*, 7541. (b) Anderson, A. B.; Debnath, N. C. *J. Phys. Chem.* **1983**, *87*, 1938.
(4) Fielder, W. L.; Stearns, C. A.; Kohl, F. J.; Fyburg, G. C. "Formation of Na_2SO_4(c) from NaCl(c), SO_2(g) and O_2(g)"; International Conference on High-Temperature Corrosion, San Diego, CA, March 2–6, 1981.
(5) Kohl, F. J.; Fielder, W. L.; Stearns, C. A., private communication.
(6) See ref 3a; for H a 1s orbital exponent of 1.2 au and ionization potential of 12.6 eV are used.
(7) See a freshman chemistry text. An early reference is the following: Goodeve, C. F.; Eastman, A. S.; Dooley, A. *Trans. Faraday Soc.* **1937**, *30*, 1127.
(8) Sievert, R.; Castleman, A. W., Jr. *J. Phys. Chem.* **1984**, *88*, 3329.
(9) Holland, P. M.; Castleman, A. W., Jr. *Chem. Phys. Lett.* **1978**, *56*, 51.

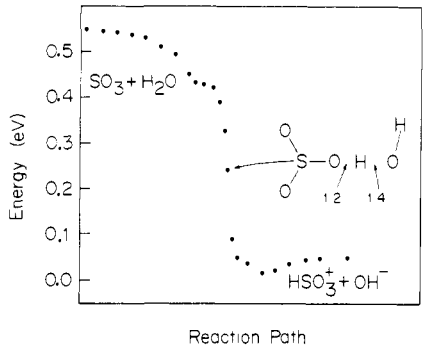

Figure 4. Energy along the reaction pathway (minimum energy path over energy surface as a function of the SO–H and HO–H distances) for the $H_2O + SO_3 \rightarrow HSO_3^+ + OH^-$ reaction.

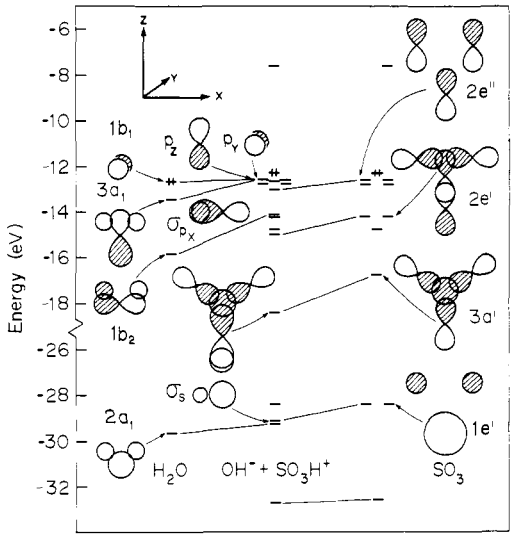

Figure 5. Correlations of H_2O and SO_3 molecular orbitals with those for OH^- and SO_3H^+.

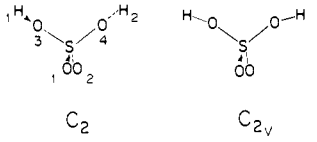

Figure 6. Optimized C_2 and C_{2v} structures for H_2SO_4.

overlap in the transition state; orbitals labeled 2 and 3 indicate the transfer is symmetry forbidden. It is noted that the scaled CNDO result of 14 kJ/mol for the activation energy is much smaller, but this is difficult to justify on the basis of molecular orbital bonding arguments. The CNDO method often strongly overestimates bonding stabilizations.

A pathway to hydrogen sulfate formation which has no activation energy barrier has a proton transferred from water to an oxygen atom in SO_3 in a linear arrangement (see Figure 4):

$$(O_2)S—O\cdots H\cdots O(H) \rightarrow [(O_2)S—OH]^+ + [OH]^- \quad (5)$$

This intermediate shows a stability of 58 kJ/mol with respect to gas-phase water and sulfur trioxide. Stabilization of the SO_3 3a′ orbital due to overlap with the H 1s orbital dominates although there is also stabilization in the e orbitals, as shown in Figure 5. The ion pair rearranges with no activation energy barrier, forming hydrogen sulfate. The orbital correlation diagram is in Figure 3. The calculated stability gain for forming a gas-phase sulfuric acid molecule from water and sulfur trioxide is 133 kJ/mol for the C_{2v} structure (Figure 6) and 130 kJ/mol for the C_2 structure, somewhat greater than 97 kJ/mol from experiment.[10] Holland and Castleman calculated 700 kJ/mol but scaled this and their other calculated energies by 97/700.[9]

Table I. Calculated and Experimental[9] Structure Parameters for H_2SO_4 (See Figure 3)

structure parameter	C_{2v}	C_2	C_2(exptl)
R(OH), Å	1.03	1.03	0.97
$R(SO_1)$, Å	1.50	1.49	1.42
$R(SO_3)$, Å	1.48	1.50	1.57
(O_1SO_2), deg	110	112	123
(O_3SO_4), deg	107	108	101
(HO_3S), deg	161	152	108
(HO_3SO),[a] deg	0	31	21
(PP_2),[b] deg	90	89	88

[a] Dihedral angle. [b] Smaller angle of intersection of the two SO_2 planes.

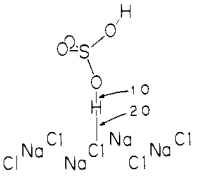

Figure 7. Structure of H_2SO_4 bonded through a hydrogen atom to the NaCl surface.

A microwave study by Kuczkowski, Suenram, and Lovas favors the C_2 structure.[11] We find the C_2 and C_{2v} structures comparable in stability in our non-self-consistent molecular orbital calculations. In the C_2 structure a weak-bonding Mulliken overlap is seen between each hydrogen atom and the oxygen atom of the opposite OH group, while overlaps with the other oxygen atoms and sulfur are negative. This is suggestive of a H^+ + lone-pair attractive electrostatic interaction which, in a self-consistent calculation, would favor the C_2 structure over C_{2v}. If the preference is weak enough, the OH groups will twirl around the S–O axes, defining cones in a series of quantized states. The calculated structures of H_2SO_4 are given in Table I, and the results for the C_2 structure are compared with the experimental results of ref 11. As is often the case with the ASED molecular orbital theory the bond lengths are within 0.1 Å and all but the HOS angles within 10° of the experimental results. The excessive HOS angle is a consequence of the lone pairs on oxygen which are not entirely properly taken into account. It may be noted that angles about oxygen are accurately predicted when other interactions dominate, as in pyrosulfate.[3a] In calculations involving water in the paper the experimental HOH angle is assumed.

Reaction of Hydrogen Sulfate with Sodium Chloride

Hydrogen sulfate is found to bond to the central chloride ion in the top layer of a square two-atom-thick Na_9Cl_9 cluster with an energy of 30 kJ/mol with a structure shown in Figure 7. In this structure a charge transfer of ~0.6 electron has taken place from the surface to the H_2SO_4 molecule. This charge will attract a sodium cation out of the surface from a site adjacent to the HCl precursor site. The barrier to this step should be zero because of the Coulombic attraction, an energy term omitted in the ASED–MO theory. As the sodium bisulfate anion forms, HCl will desorb from the surface. As may be seen in Figure 8, the HCl bonding stabilizations outweigh the loss of OH bonding stabilizations in H_2SO_4. The calculated energy to remove HSO_4^- from the surface is 32 kJ/mol, but the addition of Na^+ from the surface will make the barrier to $NaHSO_4$ formation very small because of the strong Coulombic attraction. The calculated energy to remove HCl from the surface is 48 kJ/mol which will be overcome by the entropy contribution to the free energy of desorption. This process repeats, leading to the formation of Na_2SO_4 and HCl with the same energetics. From standard thermodynamic

(10) Stull, D. R.; Prophet, H., Eds. "JANEF Thermochemical Tables", 2nd ed.; National Bureau of Standards: Washington, DC; NSRDS-NBS 37.

(11) Kuczkowski, R. L.; Suenram, R. D.; Lovas, F. J. *J. Am. Chem. Soc.* **1981**, *103*, 2561.

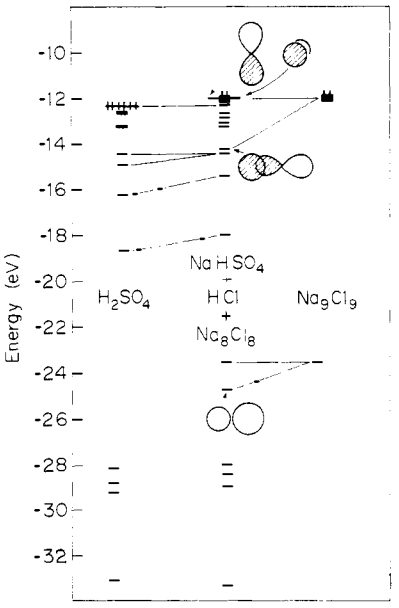

Figure 8. Correlation of H_2SO_4 and Na_9Cl_9 molecular orbitals with those for $NaHSO_4$ + HCl + Na_8Cl_8.

data,[12] the overall reaction (eq 3) is exothermic by 14 kJ/mol while we calculated 199 kJ/mol for forming molecular (not solid) sodium sulfate. The stability gain for the formation of sodium sulfate is sensitive to the energies of the sulfate acceptor orbitals relative to the chloride donor orbitals. Figure 8 shows these sets of levels are both close to −12 eV in the calculations. A reduction in reaction energy could be gained by moving the sulfate levels up or the chloride levels down. Even if the sulfate levels were moved above the chloride levels, HCl bond formation would still lead to the electron transfer to sulfate, but the heat of the reaction would be reduced. Another uncertainty is the Madelung contributions to solid sodium chloride and solid sodium sulfate, which are omitted in our model. These may serve to stabilize sodium chloride relative to the sulfate and, if included, lower the calculated heat of reaction.

From standard thermodynamic data,[12] the reaction of liquid sulfuric acid with solid sodium chloride to form solid sodium sulfate and hydrogen chloride gas is endothermic by 64 kJ/mol. Yet, this reaction dates back to Glauber in the seventeenth century and is a standard laboratory preparative procedure.[13] The reaction must be driven by the entropy of formation of 2 mol of hydrogen chloride gas.

(12) Reference 8 and the following: "CRC Handbook of Chemistry and Physics"; Weast, R. C., Ed.; CRC Press: Boca Raton, 1979.
(13) Parks, G. D., Ed. "Mellor's Modern Inorganic Chemistry"; Wiley: New York, 1967.

Conclusion

In this study no barrier to gas-phase sulfuric acid formation from the reactants sulfur trioxide and water is found. This supports the molecular beam reaction study of Sievert and Castleman.[8] While the $SO_3 \cdot H_2O$ adduct is stable by ~74 kJ/mol, hydrogen transfer to form hydrogen sulfate in this structure has too high a barrier. The transition state, which has an approximately linear O···H···O structure, is accessible during gas-phase collisions of water with SO_3. Such collisions will be of high frequency under the reaction conditions of Sievert and Castleman (353 K)[8] and Khol et al. (~600 °C).[5] Even when the adduct forms, at these temperatures entropy will cause it to fall apart after a brief time. It may be noted that for an analogous gas-phase reaction $N_2O_4(g) \rightarrow 2NO_2(g)$ the standard $T\Delta S$ contribution to ΔG is 53 kJ/mol, and a similar value may be assumed for the $SO_3 \cdot H_2O$ adduct. An alternative mechanism might involve H_2O attack on the adduct. $SO_3 \cdot H_2O$ will be unable to coordinate a second water molecule, but the same hydrogen-transfer mechanism might apply with OH displacing the water molecule. The failure to observe an adduct even at 353 K[8] makes this mechanism unlikely at the high temperature of interest here.

Once formed, the hydrogen sulfate molecule reacts with solid sodium chloride, transferring a hydrogen atom to chloride while the surface transfers an electron and a sodium cation to sulfate, yielding sodium bisulfate and hydrogen chloride. This process repeats, yielding sodium sulfate and another mole of hydrogen chloride. The reaction is well-known.[13]

Overall, our results are consistent with a zero activation energy barrier for sodium sulfate formation from sulfur trioxide, water, and sodium chloride. This supports the recent studies of Kohl et al.[5] The mechanism for this process is distinctly different from that for anhydrous conditions where a $SO_2 \cdot O_2 \cdots SO_3$ intermediate involving an $SO_2 \cdot O_2$ adduct adsorbed to the sodium chloride surface and gas-phase SO_3 is formed. At low temperature this intermediate collapses to the pyrosulfate anion[3a] which decomposes to sulfate and sulfur trioxide on heating.[3a] The mechanism determined in this paper for hydrous conditions precludes the direct formation of sodium pyrosulfate. Sulfate will form first and will take on gas-phase sulfur trioxide when at sufficient pressure to favor pyrosulfate stability. An experimental test of this hypothesis would be worthwhile.

Acknowledgment. Thanks are extended to Kathy Collen for performing most of the computer calculations. Additional help was provided by Dr. S. P. Mehandru. The advice of Drs. Williams L. Fielder, Fred J. Kohl, and Carl A. Stearns of the NASA Lewis Research Center, comments from Dr. William J. Kroenke of the B. F. Goodrich Research and Development Center, and a preprint of ref 8 from Professor W. A. Castleman, Jr., were gratefully received. The work was supported by NASA Grant NAG-3-341.

Registry No. SO_3, 7446-11-9; H_2O, 7732-18-5; H_2SO_4, 7664-93-9; NaCl, 7647-14-5.